An efficient method for the anisotropic diffusion equation in magnetic fields.

D. Muir[1] K. Duru[2] M. Hole[3] S. Hudson[4]

(Received 31 January 2023; revised 28 July 2023)

Abstract

We solve the anisotropic diffusion equation in 2D, where the dominant direction of diffusion is defined by a vector field which does not conform to a Cartesian grid. Our method uses operator splitting to separate the diffusion perpendicular and parallel to the vector field. The slow time scale diffusion (perpendicular to the vector field) is solved using a provably stable finite difference formulation, and parallel diffusion represented by an integral operator. Energy estimates are shown for the continuous and semi-discrete cases. Numerical experiments are performed showing convergence of the method, and examples are given to demonstrate the capabilities of the method.

DOI:10.21914/anziamj.v64.17966, Published 2023-10-23, as part of the Proceedings of the 20th Biennial Computational Techniques and Applications Conference. ISSN 1445-8810. (Print two pages per sheet of paper.)

Contents

1 Introduction

The anisotropic diffusion equation provides a simplified model for transport phenomena in magnetic confinement fusion devices. To confine a super heated plasma, these devices use extremely strong magnetic fields which are a few million times stronger than that of the Earth. The strength of the magnetic field results in diffusive processes being orders of magnitude faster along magnetic field lines compared to across them. The ratio of diffusion coefficients parallel and perpendicular to the field lines can exceed $\sim 10^{10}$ [4]. This disparity in diffusive scales results in numerical errors quickly polluting the solution when the computational grid is not aligned with the magnetic field lines [5].

Günter et al. [5] resolved this issue by introducing a method which depends on tracing the magnetic field lines, resulting in a field aligned form of the anisotropic diffusion equation that minimises the numerical pollution [5]. Hudson and Breslau [7] showed that isocontours of equilibrium solutions of the field aligned equation closely resemble features of the underlying field.

This suggests that solutions of the equation can provide a proxy for other properties important for the confinement of particles [7, 6, 11]. However, an equilibrium solver can be undesirable even when these steady state solutions are sought since, as the perpendicular diffusion vanishes, the problem becomes ill conditioned at best and ill-posed at worst. To resolve the issue with ill-posedness, Chacón, del-Castillo-Negrete, and Hauck [1] introduced a time dependent method using operator splitting and replaced the parallel diffusion term with an integral operator formulated in earlier work by del-Castillo-Negrete and Chacón [15].

In this article we introduce an approach to solving a field aligned form of the anisotropic diffusion equation which is provably stable and efficient. We demonstrate this on a simplified 2D version of the problem where we consider one spatial dimension lying purely parallel to the magnetic field and the other perpendicular to it. For simplicity, we replace the magnetic field with functions for the parallel map. This simplification captures many of the challenges associated with the full 3D problem and works when field line tracing is used. We derive energy estimates of the solution of the underlying initial boundary value problem (IBVP). In the perpendicular direction we approximate the diffusion equation using summation-by-parts (SBP) finite difference operators [10]. Boundary conditions and the parallel diffusion term are implemented weakly using the simultaneous approximation term (SAT). We prove numerical stability by deriving discrete energy estimates mimicking the continuous energy estimates. The numerical method can be extended to multiple dimensions and complex geometries.

This article is ordered as follows. Section 2 details the SBP formulation, which is used to discretise perpendicular to the magnetic field. Section 3 formally introduces the field aligned anisotropic diffusion equation, details the simplifications made to reduce it to one dimension by introducing an integral operator for the parallel transport, and provides a proof of well-posedness. Section 4 introduces the semi-discrete form of the anisotropic diffusion equation using the SBP with simultaneous approximation terms (SBP-SAT), and the discrete form of the parallel integral operator. We also

prove stability for the semi-discrete problem. The numerical approach for the discrete problem is outlined in Section 4.1. Numerical results are presented in Section 5. This includes demonstrating convergence by the method of manufactured solutions, followed by some examples which illustrate the effects of the parallel map and the robustness of the method. We summarise the article in Section 6.

2 Preliminaries

Here we introduce the SBP formulation, which we use to prove the stability of our scheme. More elaborate discussions are provided elsewhere [9, 8, 3, 2, 14]. We consider the spatial interval $x \in [0, L]$ and discretise it into n grid points with a uniform spatial step $\Delta x > 0$:

$$x_j = (j-1)\Delta x\,, \quad \Delta x = \frac{L}{n-1}\,, \quad j = 1, 2, \ldots, n\,.$$

Let $u : \mathbb{R}^2 \to \mathbb{R}$ be a scalar function and $\mathbf{u} = [u_1(t), u_2(t), \cdots u_n(t)]^T \in \mathbb{R}^n$ denote the semi-discrete scalar field on the grid, where $u_j(t) \approx u(x_j, t)$. The operators $D_x, D_{xx}^{(k)} \in \mathbb{R}^{n\times n}$ denote discrete approximations of the first and second spatial derivatives on the grid, that is $(D_x\mathbf{u})_j \approx \partial u/\partial x|_{x=x_j}$ and $(D_{xx}^{(k)}\mathbf{u})_j \approx \partial\left(k\partial u/\partial x\right)/\partial x|_{x=x_j}$, where the superscript $k > 0$ is the diffusion coefficient in the second derivative. Furthermore, let H be a matrix which induces a norm, inner product and quadrature rule. The discrete operators D_x and $D_{xx}^{(k)}$ are called SBP operators if

$$D_x = H^{-1}Q\,, \quad Q + Q^T = B := \mathrm{diag}([-1, 0, \ldots, 0, 1])\,, \tag{1}$$

$$H = H^T\,, \quad \mathbf{u}^T H\mathbf{u} > 0\,, \quad \forall \mathbf{u} \in \mathbb{R}^n\,, \tag{2}$$

$$D_{xx}^{(k)} = H^{-1}(-M^{(k)} + BKD_x)\,, \quad M^{(k)} = (M^{(k)})^T\,, \quad \mathbf{u}^T M^{(k)}\mathbf{u} \geqslant 0\,, \tag{3}$$

where $K = \mathrm{diag}([k(x_1), k(x_2), \cdots, k(x_n)])$. The SBP operators D_x and $D_{xx}^{(k)}$ are called *fully compatible* if

$$M^{(k)} = D_x^T(KH)D_x + R_x^{(k)}\,, \quad R^{(k)} = (R^{(k)})^T\,, \quad \mathbf{u}^T R^{(k)}\mathbf{u} \geqslant 0\,, \tag{4}$$

where $R_x^{(k)}$ is often called the remainder operator [8]. We use fully compatible and diagonal norm SBP operators with $H = \Delta x \, \mathrm{diag}([h_1, h_2, \cdots, h_n])$, where $h_j > 0$ are the weights of a composite quadrature rule. The SBP properties (1)–(3) are useful in proving numerical stability.

Remark 1. We call the operators D_x and $D_{xx}^{(k)}$ *diagonal norm* SBP operators since the matrix H which induces the norm is diagonal.

3 The anisotropic diffusion equation

The field aligned anisotropic diffusion equation [5, 7] is

$$\frac{\partial u}{\partial t} = \nabla \cdot (\kappa_\perp \nabla_\perp u) + \nabla \cdot (\kappa_\parallel \nabla_\parallel u), \tag{5}$$

where $\nabla_\parallel$ is the directional derivative along the magnetic field, $\nabla_\perp = \nabla - \nabla_\parallel$, and $\kappa_\perp > 0$ and $\kappa_\parallel > 0$ are the diffusion coefficients in the perpendicular and parallel directions, respectively. Note that $\kappa_\parallel / \kappa_\perp \gg 1$ and can exceed $\sim 10^{10}$ in many relevant applications. Equation (5) is fully 3D in space. To simplify we follow previous works outlined in Section 1, and solve equation (5) on a 2D plane in the perpendicular ($\boldsymbol{e}_1$ and $\boldsymbol{e}_2$) direction, which reduces the computational complexity significantly. The effect of the parallel diffusion is then included through an integral operator $\mathcal{P}_\parallel$. This gives

$$\frac{\partial u}{\partial t} = \nabla \cdot (\kappa_\perp \nabla_\perp u) + \mathcal{P}_\parallel u, \tag{6}$$

where

$$\nabla \cdot (\kappa_\parallel \nabla_\parallel) \sim \mathcal{P}_\parallel, \quad \Big(u, (\mathcal{P}_\parallel + \mathcal{P}_\parallel^\dagger) u\Big) \leqslant 0. \tag{7}$$

Here $\mathcal{P}_\parallel^\dagger$ is the adjoint operator of $\mathcal{P}_\parallel$ and $(\cdot, \cdot)$ denotes the standard L_2 scalar product defined on the 2D plane. The operator $\mathcal{P}_\parallel$ can be constructed explicitly, for instance with a Green's function [15, 16, 1], however we use an

interpolation approach [5, 7]. In particular, we suppose $\mathcal{P}_\parallel \propto \mathcal{P}_f + \mathcal{P}_b$, where $\mathcal{P}_f$ and $\mathcal{P}_b$ are operators which trace the solution u onto the 'forward' (positive along magnetic field) and 'backward' (negative along magnetic field) planes and also mimic the diffusive integral operators so that $\mathcal{P}_f u = w_f$, $\mathcal{P}_b u = w_b$ and $\|\mathcal{P}_f\|, \|\mathcal{P}_b\| \leqslant 1$. The purely parallel solution is then an average of the two projected values, so that $u_\parallel = (w_f + w_b)/2$.

We also make the further simplification that u is constant in $\boldsymbol{e}_2$ to reduce the number of dimensions to 2D, with solutions now in 1D. Thus (5) reduces to

$$\frac{\partial u}{\partial t} = \frac{\partial}{\partial x}\left(\kappa \frac{\partial u}{\partial x}\right) + \mathcal{P}_\parallel u, \quad x \in [0, L], \quad \kappa = \kappa_\perp > 0, \tag{8}$$

with smooth initial condition

$$u(x, 0) = f(x). \tag{9}$$

For simplicity we also only consider the case of Neumann boundary conditions

$$\kappa \left.\frac{\partial u}{\partial x}\right|_{x=0} = g(t), \quad \kappa \left.\frac{\partial u}{\partial x}\right|_{x=L} = g(t). \tag{10}$$

To simplify the analysis we assume no-flux boundary conditions, where $g(t) = 0$. However, the analysis can be extended to non-homogeneous boundary data, $g(t) \neq 0$. The numerical experiments in Section 5 verify that the analysis is true for non-homogeneous data. The following theorem proves the well-posedness of the simplified problem.

Theorem 2. *Consider the anisotropic diffusion equation* (8) *subject to the smooth initial condition* (9) *and Neumann boundary conditions* (10). *If* $\left(u, (\mathcal{P}_\parallel + \mathcal{P}_\parallel^\dagger)u\right) \leqslant 0$, *then*

$$\frac{d}{dt}\|u\|^2 \leqslant 0.$$

Proof: We use the energy method; that is, we multiply (8) with the solution u and integrate over the domain:

$$\int_0^L u\frac{\partial u}{\partial t}dx = \int_0^L u\frac{\partial}{\partial x}\left(\kappa\frac{\partial u}{\partial x}\right)dx + \int_0^L u\mathcal{P}_\parallel u dx\,. \tag{11}$$

Integration by parts gives

$$\frac{1}{2}\frac{d}{dt}\int_0^L u^2 dx = -\int_0^L \frac{\partial u}{\partial x}\kappa\frac{\partial u}{\partial x}dx + \left[u\kappa\frac{\partial u}{\partial x}\right|_0^L + \int_0^L u\mathcal{P}_\parallel u dx\,. \tag{12}$$

Enforcing the boundary conditions (10) eliminates the second term on the right. Adding the conjugate transpose of (12) gives

$$\frac{d}{dt}\|u\|^2 = -2\int_0^L \frac{\partial u}{\partial x}\kappa\frac{\partial u}{\partial x}dx + \int_0^L u\left(\mathcal{P}_\parallel + \mathcal{P}_\parallel^\dagger\right)u dx \leqslant 0\,. \tag{13}$$

♠

To ensure stability of the numerical method we seek to mimic the energy estimate (13) at the discrete level.

4 Numerical approach

We follow the method of lines by discretising the spatial variable while leaving the time variable continuous. We approximate the spatial derivative using SBP operators [9], while the boundary conditions and the parallel operator are implemented weakly using penalties. The semi-discrete approximation of the anisotropic diffusion equation (8) using the SBP-SAT method is

$$\frac{d\mathbf{u}}{dt} = D_{xx}^{(k)}\mathbf{u} + \text{SAT} + P_\parallel\mathbf{u}\,, \quad \mathbf{u}(0) = \mathbf{f}\,, \tag{14}$$

where $D_{xx}^{(k)}$ is the SBP operator given in (3) and

$$P_\parallel = \frac{\tau_\parallel}{2}H^{-1}\kappa_\parallel\overbrace{\left(I - \frac{1}{2}[P_f + P_b]\right)}^{A_\parallel}, \quad \text{SAT} = \tau_0 H^{-1}B\left(KD_x\mathbf{u} - \mathbf{g}\right), \tag{15}$$

are weak numerical implementations of the parallel diffusion operator (7) and the boundary conditions (10), and where $\tau_{\parallel}$ and τ_0 are penalty parameters to be determined for stability. Boundary data is given by $\mathbf{g} = [g_1(t), 0, \dots, 0, g_N(t)]^T$. The matrices P_f and P_b are projection operators. Future work will provide more detail on the construction of these operators. Before showing stability we first prove the following lemma regarding the definiteness of the numerical parallel diffusion operator.

Lemma 3. *Consider the numerical parallel diffusion operator*

$$P_{\parallel} = \tfrac{\tau_{\parallel}}{2} H^{-1} \kappa_{\parallel} A_{\parallel}\,, \quad A_{\parallel} = I - \tfrac{1}{2}(P_f + P_b)\,, \tag{16}$$

with $\kappa_{\parallel} \geqslant 0$, $\tau_{\parallel} = \alpha/\Delta x$ *and* $\alpha \leqslant 0$. *If* $\|P_f\| \leqslant 1$ *and* $\|P_b\| \leqslant 1$ *then*

$$\mathbf{u}^T(A_{\parallel} + A_{\parallel}^T)\mathbf{u} \geqslant 0\,, \quad \mathbf{u}^T\left[(HP_{\parallel}) + (HP_{\parallel})^T\right]\mathbf{u} \leqslant 0\,, \quad \forall \mathbf{u} \in \mathbb{R}^n\,.$$

Proof: The sum $A_{\parallel} + A_{\parallel}^T$ is symmetric. Since $\|P_f\|$ and $\|P_b\| \leqslant 1$, it follows that $\mathbf{u}^T\left(2I - \frac{1}{2}\left[(P_f + P_f^T) + (P_b + P_b^T)\right]\right)\mathbf{u} = \mathbf{u}^T(A_{\parallel} + A_{\parallel}^T)\mathbf{u} \geqslant 0$. Therefore choosing $\alpha < 0$ gives $\mathbf{u}^T\left[(HP_{\parallel}) + (HP_{\parallel})^T\right]\mathbf{u} = \frac{\kappa_{\parallel}\alpha}{2\Delta x}\mathbf{u}^T(A_{\parallel} + A_{\parallel}^T)\mathbf{u} \leqslant 0$. ♠

We now prove the stability of the semi-discrete approximation (14).

Theorem 4. *Consider the semi-discrete approximation* (14) *for homogeneous boundary data* $\mathbf{g} = 0$ *where the numerical parallel diffusion operator* $P_{\parallel}$ *and the* SAT *are given by* (15), *with* $\tau_{\parallel} = \alpha/\Delta x \leqslant 0$ *and* $\tau_0 = -1$. *Let* $\|\mathbf{u}\|_H^2 = \mathbf{u}^T H \mathbf{u}$, *if* $\|P_f\| \leqslant 1$ *and* $\|P_b\| \leqslant 1$ *then*

$$\frac{d}{dt}\|\mathbf{u}\|_H^2 \leqslant 0\,, \quad \forall \mathbf{u} \in \mathbb{R}^n\,.$$

Proof: Multiply (14) from the left by $\mathbf{u}^T H$ to obtain

$$\mathbf{u}^T H \frac{d\mathbf{u}}{dt} = -\mathbf{u}^T(M^{(\kappa)} + BKD_x)\mathbf{u} + \tau_0 \mathbf{u}^T BKD_x \mathbf{u} + \mathbf{u}^T H P_{\parallel}\mathbf{u}\,. \tag{17}$$

Choosing $\tau_0 = -1$ and adding the transpose of the products gives

$$\frac{d}{dt}\|\mathbf{u}\|_H^2 = -2\mathbf{u}^T M^{(\kappa)}\mathbf{u} + \mathbf{u}^T\left[(HP_\parallel) + (HP_\parallel)^T\right]\mathbf{u} \leqslant 0\,. \tag{18}$$

♠

4.1 The fully-discrete approximation

We discretise the time variable $t_{l+1} = t_l + \Delta t$ with the time-step $\Delta t > 0$ where $t_0 = 0$ and $l = 0, 1, 2, \ldots$. The fully discrete solution at the time level $t_l > 0$ is denoted by $\mathbf{u}^l$ with $\mathbf{u}^0 = \mathbf{f}$. Solving the fully discrete version of the semi-discrete anisotropic diffusion equation (14) is performed by operator splitting. This results in a two stage solution is

$$(I + \Delta t H^{-1} M_x^{(k)})\mathbf{u}^{l+\frac{1}{2}} = \mathbf{u}^l + \Delta t \mathbf{F}(t_{l+1})\,, \quad \mathbf{F}(t_{t_{l+1}}) = \tau_0 H^{-1} B\mathbf{g}(t_{l+1})\,, \tag{19}$$

$$\boldsymbol{w}_f^{l+\frac{1}{2}} = P_f\mathbf{u}^{l+\frac{1}{2}}\,, \quad \boldsymbol{w}_b^{l+\frac{1}{2}} = P_b\mathbf{u}^{l+\frac{1}{2}}\,, \tag{20}$$

$$\mathbf{u}^{l+1} = \mathbf{u}^{l+\frac{1}{2}} + \frac{\Delta t \tau_\parallel \kappa_\parallel}{2} H^{-1}\left(\mathbf{u}^{l+1} - \frac{1}{2}[\boldsymbol{w}_f^{l+\frac{1}{2}} + \boldsymbol{w}_b^{l+\frac{1}{2}}]\right). \tag{21}$$

The first stage is the perpendicular solution using the backward Euler approximation and involves solving an elliptic linear system which can be solved efficiently by the conjugate gradient method. Stage two, which includes (20) and (21), propagates the parallel diffusion and can be computed directly.

5 Numerical results

We first demonstrate the convergence of the SBP-SAT scheme (without a parallel component) by the method of manufactured solutions [13, 12]. We choose the manufactured solution, with exact solution

$$u(x, t) = \cos(2\pi t)\sin(17\pi x + 1)\,. \tag{22}$$

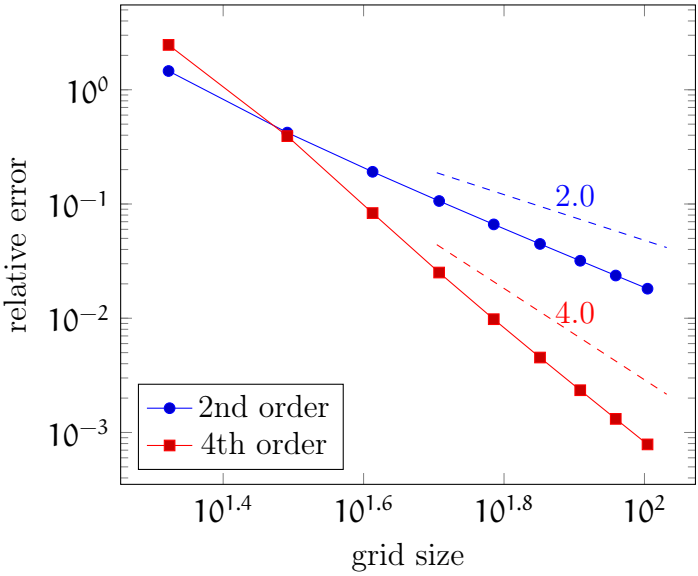

Figure 1: Convergence rates for second (blue) and fourth (red) order SBP operators with first order time solver. Dashed lines are references lines and have the expected slopes for associated convergence rates.

The convergence results are shown in Figure 1. We set a fixed time step of $\Delta t = \Delta x^2/100$. Comparison with the (dashed) reference lines shows both slightly over-perform their expected convergence rate with $\sim \mathcal{O}(h^{2.5})$ for the second order, and $\sim \mathcal{O}(h^{4.5})$ for the fourth order.

5.1 Examples

We now present examples of the field aligned 1D anisotropic diffusion equation which demonstrate the effect of the the parallel operator on the solution. These are shown in Figures 2 and 3. In all cases the boundary conditions are no flux, $\partial_x u|_{x=0} = \partial_x u|_{x=1} = 0$, and the diffusion coefficients in the perpendicular and parallel directions are $\kappa_\perp = 10^{-3}$ and $\kappa_\parallel = 1$.

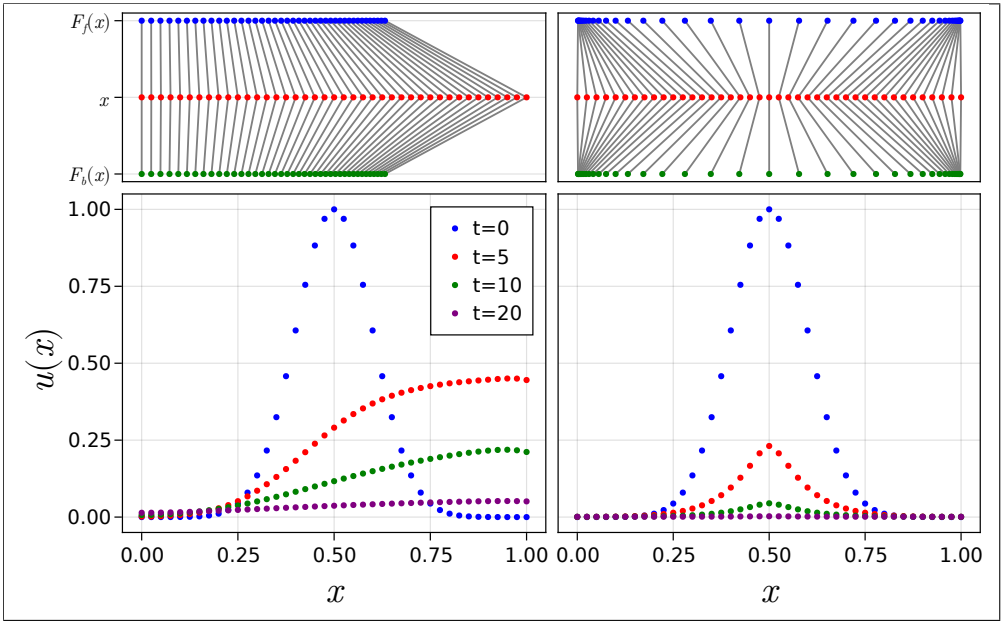

Figure 2: Top left: Parallel mapping given by F_1 in equation (24). Bottom left: Solution to (8) at various times with parallel map given by equation F_1 in (24). Top right: point mapping as per F_2 in (24). Bottom right: Solution to (8) at various times with parallel map given by equation F_2 in (24).

The initial condition for the example in Figure 2 is a Gaussian:

$$u(x,0) = \exp\left(\frac{-(x-0.5)^2}{0.02}\right). \tag{23}$$

The parallel maps in the forward and backward directions are

$$F_1(x) = 1 - \exp(-x) \quad \text{and} \quad F_2(x) = \tfrac{1}{2}[\tanh(2\pi x - \pi) + 1], \tag{24}$$

respectively. The point mappings of F_1 and F_2 are visualised in the top row of Figure 2.

Solutions in Figure 2 tend towards a uniform value, as expected with no-flux boundaries. Given the point mapping by F_1, we see the right hand side of

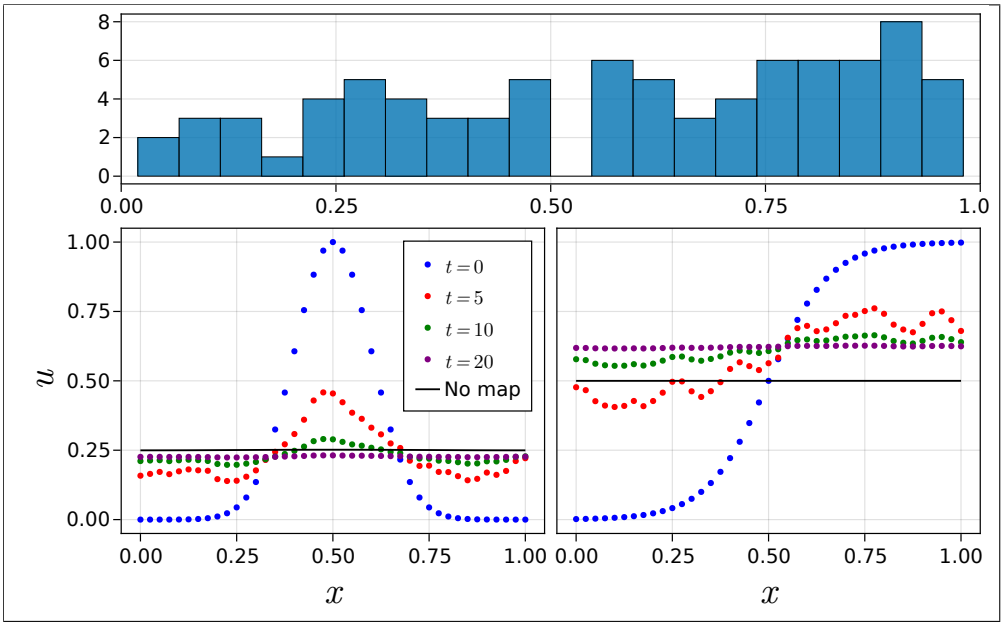

Figure 3: Top: Distribution of points on forward and backward planes, showing a slight bias towards the right side of the domain. Bottom left: Evolution of solution with random point mapping and initial condition specified by F_1 in (24). Bottom right: Same as right figure, but initial condition given by F_2 in (24). The black line in the lower figures corresponds to the 1D solution without parallel mapping.

the solution maps to the centre of the Gaussian profile, which explains the larger $\mathfrak{u}$ for larger $\mathfrak{x}$ values seen in the lower left plot of Figure 2 . The point mapping by F_2 diffuses into low $\mathfrak{u}$ regions, quickly flattening out the solution.

The example in Figure 3 demonstrates both the robustness of the approach and the effect of the operator on a standard 1D solution to the equation. Here the forward and backward maps randomly map points in the domain. The parallel maps F_1 and F_2 in (24) are now used as the initial conditions in the left and right plots of Figure 3, respectively.

Solutions are again uniform, as expected, and are compared to a solution with no parallel mapping (black line). They deviate from the no parallel mapping solution because the parallel map has a slight bias towards the right side of the domain, as shown in the bar plots at the top of Figure 3. In the case of the Gaussian on the left of Figure 3, this results in diffusion from the high $\mathfrak{u}$ into the low $\mathfrak{u}$ region, reducing the final state of the solution. In the sigmoid function, on the right of Figure 3, points are mapped into the high $\mathfrak{u}$ region, resulting in a slightly higher final solution than the no parallel mapping case.

6 Conclusions

We have derived a stable and efficient numerical operator splitting technique to solve the anisotropic diffusion equation in a two dimensional geometry not aligned with a regular mesh. We achieve this with the use of SBP with SAT in the perpendicular solution and an integral operator for the parallel solution. The time steps are evolved by using an implict Euler conjugate gradient method.

Our method produces accurate results, verified by the method of manufactured solutions. The results show the SBP-SAT method outperforms the expected second and fourth order convergence rates. Examples show our method solving the field aligned anisotropic diffusion equation with a variety of parallel maps. Moreover, the random point mapping examples shows our approach is robust.

Future work will extend this method to two-dimensional planes in the perpendicular direction and use parallel maps given by systems of ordinary differential equations. Specifically we will be interested in extending the method to geometry provided by real magnetic fields.

References

[1] L. Chacón, D. del-Castillo-Negrete, and C. D. Hauck. “An asymptotic-preserving semi-Lagrangian algorithm for the

time-dependent anisotropic heat transport equation". In: *J. Comput. Phys.* 272 (2014), pp. 719–746. DOI: 10.1016/j.jcp.2014.04.049. (Cit. on pp. C18, C20).

[2] D. C. Del Rey Fernández, J. E. Hicken, and D. W. Zingg. "Review of summation-by-parts operators with simultaneous approximation terms for the numerical solution of partial differential equations". In: *Comput. Fluids* 95 (2014), pp. 171–196. DOI: 10.1016/j.compfluid.2014.02.016 (cit. on p. C19).

[3] K. Duru and K. Virta. "Stable and high order accurate difference methods for the elastic wave equation in discontinuous media". In: *J. Comput. Phys.* 279 (2014), pp. 37–62. DOI: 10.1016/j.jcp.2014.08.046 (cit. on p. C19).

[4] R. Fitzpatrick. "Helical temperature perturbations associated with tearing modes in tokamak plasmas". In: *Phys. Plasmas* 2.3 (1995), pp. 825–838. DOI: 10.1063/1.871434 (cit. on p. C17).

[5] S. Günter, Q. Yu, J. Krüger, and K. Lackner. "Modelling of heat transport in magnetised plasmas using non-aligned coordinates". In: *J. Comput. Phys.* 209.1 (2005), pp. 354–370. DOI: 10.1016/j.jcp.2005.03.021. (Cit. on pp. C17, C20, C21).

[6] P. Helander, S. R. Hudson, and E. J. Paul. "On heat conduction in an irregular magnetic field. Part 1". In: *J. Plasma Phys.* 88.1, 905880122 (Feb. 2022). DOI: 10.1017/S002237782100129X. (Cit. on p. C18).

[7] S. R. Hudson and J. Breslau. "Temperature contours and ghost surfaces for chaotic magnetic fields". In: *Phys. Rev. Lett.* 100.9, 095001 (2008). DOI: 10.1103/PhysRevLett.100.095001. (Cit. on pp. C17, C18, C20, C21).

[8] K. Mattsson. "Summation by parts operators for finite difference approximations of second-derivatives with variable coefficients". In: *J. Sci. Comput.* 51.3 (2012), pp. 650–682. DOI: 10.1007/s10915-011-9525-z (cit. on pp. C19, C20).

[9] K. Mattsson and J. Nordström. "Summation by parts operators for finite difference approximations of second derivatives". In: *J. Comput. Phys.* 199.2 (2004), pp. 503–540. DOI: 10.1016/j.jcp.2004.03.001. (Cit. on pp. C19, C22).

[10] J. Nordström and T. Lundquist. "Summation-by-parts in time: The second derivative". In: *SIAM J. Sci. Comput.* 38.3 (2016), A1561–A1586. DOI: 10.1137/15M103861X. (Cit. on p. C18).

[11] E. J. Paul, S. R. Hudson, and P. Helander. "Heat conduction in an irregular magnetic field. Part 2. Heat transport as a measure of the effective non-integrable volume". In: *J. Plasma Phys.* 88.1, 905880107 (2022). DOI: 10.1017/S0022377821001306. (Cit. on p. C18).

[12] P. J. Roache. "Code verification by the method of manufactured solutions". In: *J. Fluids Eng.* 124.1 (2002), pp. 4–10. DOI: 10.1115/1.1436090. (Cit. on p. C24).

[13] S. Steinberg and P. J. Roache. "Symbolic manipulation and computational fluid dynamics". In: *J. Comput. Phys.* 57.2 (1985), pp. 251–284. DOI: 10.1016/0021-9991(85)90045-2. (Cit. on p. C24).

[14] M. Svärd and J. Nordström. "Review of summation-by-parts schemes for initial-boundary-value problems". In: *J. Comput. Phys.* 268 (2014), pp. 17–38. DOI: 10.1016/j.jcp.2014.02.031 (cit. on p. C19).

[15] D. del-Castillo-Negrete and L. Chacón. "Local and nonlocal parallel heat transport in general magnetic fields". In: *Phys. Rev. Lett.* 106.19, 195004 (2011). DOI: 10.1103/PhysRevLett.106.195004. (Cit. on pp. C18, C20).

[16] D. del-Castillo-Negrete and L. Chacón. "Parallel heat transport in integrable and chaotic magnetic fields". In: *Phy. Plasmas* 19.5, 056112 (2012). DOI: 10.1063/1.3696054. (Cit. on p. C20).

Author addresses

1. **D. Muir**, Mathematical Sciences Institute, Australian National University, Australian Capital Territory 2601, Australia.
mailto:dean.muir@anu.edu.au
orcid:0000-0003-1311-9273

2. **K. Duru**, Mathematical Sciences Institute, Australian National University, Australian Capital Territory 2601, Australia.
mailto:kenneth.duru@anu.edu.au
orcid:0000-0002-5260-7942

3. **M. Hole**, Mathematical Sciences Institute, Australian National University, Australian Capital Territory 2601, Australia.
mailto:matthew.hole@anu.edu.au
orcid:0000-0002-9550-8776

4. **S. Hudson**, Princeton Plasma Physics Laboratory, New Jersey,
mailto:shudson@pppl.gov
orcid:0000-0003-1530-2733